

Enantioselective Synthesis of Tungsten Trimetallic Cluster Chalcogenides

Eva M^a Guillamón,^a Marta Blasco,^a Rosa Llusar^{,a}*

^a Departament de Química Física i Analítica, Universitat Jaume I, Av. Sos Baynat s/n, 12071 Castelló, Spain

AUTHOR EMAIL ADDRESS: * author for correspondence: rosa.llusar@uji.es

CORRESPONDING AUTHOR

^a Dept. de Química Física i Analítica, Universitat Jaume I, Av. Sos Baynat s/n, 12071 Castelló, Spain: E-mail: rosa.llusar@uji.es; Tel: +34 964728086; Fax: +34 964728066; Homepage: <http://www.grupo-rllusar.uji.es>

Abstract

Excision of $\{W_3Q_7Br_4\}_n$ ($Q = S, Se$) of polymeric phases using chiral diphosphines is a general procedure to synthesize optically pure trinuclear clusters. Chiral transfer from the enantiomerically pure diphosphines (+)-1,2-bis[2,5-(dimethylphospholan-1-yl)]ethane, (*R,R*)-Me-BPE, (-)-1,2-bis[2,5-(dimethylphospholan-1-yl)]ethane, (*S,S*)-Me-BPE, and (-)-1,2-bis[2,5-(dimethylphospholan-1-yl)]benzene, (*R,R*)-DUPHOS, to the inorganic phase affords enantiopure $P-[W_3S_4Br_3((R,R)\text{-Me-BPE})_3]^+$, $M-[W_3S_4Br_3((S,S)\text{-Me-BPE})_3]^+$ (*M-1*⁺), $P-[W_3Se_4Br_3((R,R)\text{-Me-BPE})_3]^+$ (*P-2*⁺) and $P-[W_3S_4Br_3((R,R)\text{-DUPHOS})_3]^+$ (*P-3*⁺) clusters. The central $W_3(\mu_3\text{-Q})(\mu\text{-Q})$ unit defines an incomplete cuboidal core with the capping chalcogen lying on a three-fold axis and an effective C_3 symmetry. Symbols *P*- and *M*- are used to indicate the rotation of the bromine atoms around the C_3 axis, with the chalcogen atom pointing towards the viewer. Invariably, *P*- W_3Q_4 complexes are obtained starting from (*R,R*)-diphosphines, while its *M*- W_3Q_4 enantiomer is isolated in the presence of (*S,S*)-diphosphines. All complexes have been structurally characterized by single crystal X-ray diffraction and its enantiomeric character confirmed by CD spectroscopy.

Keywords

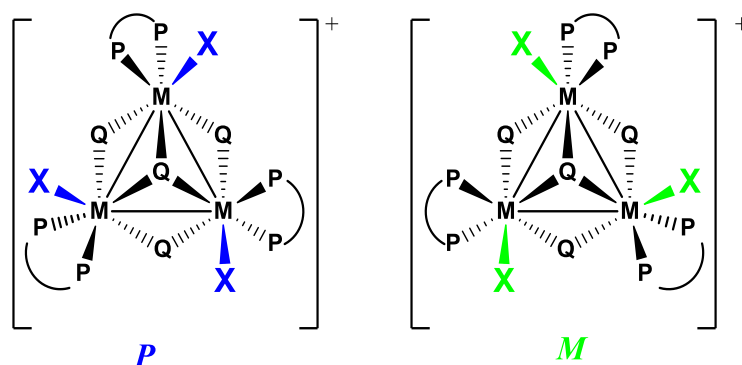
Chirality · trimetallic clusters · diphosphine ligands · tungsten · chalcogen

1. Introduction

Cuboidal transition-metal clusters constitute a large family of multimetallic compounds present in both industrial and biological catalytic processes. In particular, molybdenum and tungsten heterometallic $M_3M'S_4$ (M' = transition metal) sulfides have been proposed as models for metalloenzymes [1] or industrial hydrosulfurization (M' = Ni or Co) catalysts [2, 3]. Hidai *et al.* have recently reviewed the main catalytic functions of cubane-type transition metal M_4S_4 compounds in different areas of chemistry and, as expected, their catalytic activity is closely related to the nature of the heterometal M' . Thereby, Mo_3PdS_4 [4] and Mo_3NiS_4 clusters [5] catalyze the stereoselective addition of alcohols or carboxylic acids to electron-deficient alkynes, while Mo_3RuS_4 complexes are efficient catalysts in the cleavage of the N-N hydrazine bond [6]. Our group has also shown that Mo_3CuS_4 clusters catalyze the intra- and intermolecular cyclopropanation of diazo compounds although enantioselectivity is only moderate [7, 8]. In addition, trimetallic molybdenum and tungsten M_3S_4 ($M = Mo, W$) complexes are efficient catalyst in the selective hydrodefluorination of pentafluoropyridine in the *para* position [9] while Mo_3S_4 compounds catalyze the selective conversion of aromatic nitro derivatives to their corresponding anilines [10]. In spite of all applications found for cubane-type M_3S_4 and $M_3M'S_4$ complexes as catalysts, their role in asymmetric processes is very limited due to the scarce number of optically pure cuboidal complexes [11-13].

Along the years we have prepared and isolated a large number of molybdenum and tungsten diphosphino clusters of formula $[M_3Q_4X_3(\text{diphosphine})_3]^+$ ($M=Mo, W$; $Q=S, Se$; $X=Cl, Br, H, OH, HS$; diphosphine=dmpe, dppe, dhmpe, dhprpe, dhbupe, Me-BPE, TTF-dppe) [14-21]. The specific coordination of the bidentate ligand to the incomplete cubane-type M_3S_4 unit, with one phosphorus atom located *trans* to the capping sulfur and the other *trans* to the bridging sulfur, results in C_3 -symmetry trimetallic complexes with backbone chirality, as represented in Scheme 1. In these cluster compounds, the three metal centers are stereogenic so that, *P* (clockwise) and *M*

(anticlockwise) descriptors are used to assign the absolute configuration. Obviously, in the absence of an optically pure source, these complexes are obtained as racemic mixtures. In recent years, chirality has become a pursued and demanded property since most drugs, fertilizers or flavors are obtained from asymmetric catalyzed reactions [22-24]. In this context, the synthesis of optically pure cuboidal complexes continues to be a challenge.



Scheme 1

Chiral coordination complexes and assemblies can be generated in numerous ways. However, general strategies to afford enantiopure inorganic complexes are still much less developed from those regarding enantiopure organic substrates as stereochemistry at the metal center remains unpredictable [25-27]. In order to afford optically active trinuclear M_3S_4 units, two different approaches can be considered. The first one consists in the resolution of the racemic mixtures *via* association with a chiral shift counterion, such as TRISPHAT (tris(tetrachlorobenzenediolato)phosphate-(V)), which gives rise to the formation of supramolecular structures [28]. The success of this methodology lies in the configurational stability of the cluster cation at room and high temperatures. All attempts to resolve racemic $[Mo_3S_4Cl_3(dppe)_3]^+$ cation mixtures by association with enantiopure Δ - or Λ TRISPHAT anions were unsuccessful [29]. The second strategy is based on the transfer of chiral information into the metal center through the use of organic ligands whose configuration can be easily controlled. Our group has been able to prepare a family of enantiomerically pure Mo_3Q_4 ($Q = S, Se$) clusters through a controlled stereoisomeric excision of polymeric $\{Mo_3Q_7X_2X_{4/2}\}_n$ ($X = Cl, Br$) phases in the presence of the (+)-1,2-bis[2,5-

(dimethylphospholan-1-yl)]ethane ((*R,R*)-Me-BPE)) or (-)-1,2-bis[2,5-(dimethylphospholan-1-yl)]ethane ((*S,S*)-Me-BPE) chiral diphosphines. This strategy has been also extended to tungsten with the isolation of the *P*-[W₃S₄X₃((*R,R*)-Me-BPE)₃]⁺ (X = Br, H) bromide and hydride cations [18]. Incidentally, these Mo₃Q₄ and W₃Q₄ trimetallic clusters can act as metalloligands in front of a second transition metal to afford heterometallic M₃M'Q₄ (M' = transition metal) cubane-type compounds [30].

Motivated by the limited number of examples of enantiomerically pure [W₃Q₄X₃(diphosphine)₃]⁺ complexes, we explore in this work the generality of the excision reaction of polymeric {W₃Q₇Br₂Br_{4/2}}_n phases with chiral diphosphines, as a rational route to access enantiopure cuboidal [W₃Q₄X₃(diphosphine)₃]⁺ clusters. The (*R,R*)-DUPHOS ((-)-1,2-bis[2,5-(dimethylphospholan-1-yl)]benzene) diphosphine has been employed for the first time as excision agent and selenide polymeric phases are also excellent precursors for the isolation of optically pure W₃Se₄ complexes. The new complexes have been fully characterized by spectroscopic and spectrometric techniques and their crystal structures determined by single crystal X-ray diffraction experiments.

2. Experimental section

2.1. General methods and materials

All reactions were carried out under a nitrogen atmosphere using standard Schlenk techniques. The polymeric {W₃Q₇Br₄}_n phases were prepared according to literature methods [31, 32]. The remaining reactants were obtained from commercial sources. Solvents were dried and degassed by standard methods before use. Chromatographic work was performed by using silica gel (60Å). ³¹P{¹H} NMR spectra were recorded on a Varian-Mercury 300 MHz spectrometer using CD₂Cl₂ as solvent. The chemical shift is denoted as δ(ppm), referenced to external 85% H₃PO₄ and to the residual solvent signal. Electrospray ionization mass spectra (ESI-MS) were recorded on a Micromass Quattro LC instrument at 15-20V using dichloromethane as solvent. The chemical

composition of each peak was assigned by comparison of the isotope experimental pattern with that calculated using the MassLynx NT set program [33]. Circular dichroism measurements were recorded on a JASCO J-810 spectropolarimeter and UV/Vis measurements were carried out by using a Cary 60 spectrometer. The sample solutions were prepared in a quartz cuvette of 1 cm path length and measured at 25°C. Elemental analysis was performed in a Euro EA 3000 CHN equipment.

2.2. Synthesis

2.2.1. Synthesis of $M-[W_3S_4Br_3((S,S)\text{-Me-BPE})_3]Br \cdot 3C_7H_8$, $[M-1]Br \cdot 3C_7H_8$

To a suspension of the $\{W_3S_7Br_4\}_n$ polymeric phase (152 mg, 0.139 mmol) in dry acetonitrile (20 mL) was added (*S,S*)-Me-BPE (170 μ L, 0.625 mmol). The mixture was refluxed for 24 hours and then, the blue suspension was filtered at room temperature. The filtrate was taken to dryness under vacuum and the solid was dissolved in dichloromethane. Addition of 30 mL of ether caused the complete precipitation of a blue solid (106 mg, 37%) which was washed with 25 mL of a toluene/acetone mixture (95:5).

$^{31}P\{^1H\}$ NMR (121.47 MHz, CD_2Cl_2): $\delta=31.65$ (dd, 3P), 35.88 ppm (dd, 3P) (AA'A''BB'B'' system); UV/Vis ($1.15 \cdot 10^{-4}$ M, CH_2Cl_2): λ (ϵ) = 364 (9165), 325 (13982), 278 nm (23134 mol $^{-1}$ ·dm 3 ·cm $^{-1}$); ESI-MS (CH_2Cl_2 , 20 V) m/z: 1694 $[M]^+$; elemental analysis calcd (%) for $W_3S_4Br_4P_6C_{63}H_{108}$: C 36.90, H, 5.31; Found: C 36.3, H 5.2; CD ($1.15 \cdot 10^{-4}$ M, CH_2Cl_2) λ (mdeg): 524 (30), 404 (62), 325 (-88), 292 (21), 270 (-132), 243 nm (-85).

2.2.2. Synthesis of $P-[W_3Se_4Br_3((R,R)\text{-Me-BPE})_3](PF_6)$, $[P-2]PF_6$

The chiral diphosphine (*R,R*)-Me-BPE (102 mg, 0.395 mmol) was added to a suspension of $\{W_3Se_7Br_4\}_n$ (125 mg, 0.088 mmol) in dry acetonitrile and refluxed for 24 hours. In this case, when the filtrate was taken to dryness under vacuum, the solid was dissolved in dichloromethane and a counterion change was carried out by column chromatography. The compound was adsorbed in a silica gel column and was first washed with 200 mL acetone. Then, it was eluted with a saturated KPF_6 solution in acetone, affording a green-turquoise solution. The solution collected was taken to

dryness under vacuum and the solid was dissolved in dichloromethane. Addition of ether (30 mL) caused the complete precipitation of a green-turquoise solid (160 mg, 94%).

$^{31}\text{P}\{^1\text{H}\}$ NMR (121.47 MHz, CD_2Cl_2): δ : -143.87 (sept, 1P, $^1\text{J}_{\text{P-F}} = 704.0$ Hz), 29.37 (d, 3P, $^2\text{J}_{\text{P-Pgem}} = 6.75$ Hz), 38.83 (d, 3P, $^2\text{J}_{\text{P-Pgem}} = 6.12$ Hz); UV/Vis ($1.05 \cdot 10^{-4}$ M, CH_2Cl_2) : λ (ϵ) = 635 (1050), 383 (8771.06), 340 (13013), 291 (18960), 237 nm ($32953 \text{ mol}^{-1} \cdot \text{m}^3 \cdot \text{cm}^{-1}$); ESI-MS (CH_2Cl_2 , 20 V) m/z: 1882.2 $[\text{M}]^+$; elemental analysis, Calcd (%) for $\text{W}_3\text{Se}_4\text{Br}_3\text{P}_7\text{F}_6\text{C}_{42}\text{H}_{84}$: C 24.88, H, 4.18; Found: C 24.64, H 4.31. CD ($1.05 \cdot 10^{-4}$ M, CH_2Cl_2) λ (mdeg): 667 (20), 448 (-52), 380 (59), 339 (114), 308 (-57), 286 (173), 259 nm (205)

2.2.3. Synthesis of $P\text{-}[\text{W}_3\text{S}_4\text{Br}_3((R,R)\text{-Me-DUPHOS})_3]\text{Br} \cdot \text{C}_7\text{H}_8$, $[P\text{-}3]\text{Br} \cdot \text{C}_7\text{H}_8$

The $\{\text{W}_3\text{S}_7\text{Br}_4\}_n$ polymeric phase (200 mg, 0.183 mmol) was suspended in dry acetonitrile (25 mL) and was added (*R,R*)-Me-DUPHOS (251 mg, 0.822 mmol). The mixture was refluxed for 48 hours and then, the purple suspension was filtered. The filtrate was taken to dryness under vacuum and the solid was dissolved in dichloromethane. Addition of ether (40 mL) led to the complete precipitation of a purple solid (240 mg, 65 %) which was washed with a toluene/acetone mixture (97:3) and benzene (5mL).

$^{31}\text{P}\{^1\text{H}\}$ NMR (121.47 MHz, CD_2Cl_2): δ =34.88 (d, 3P), 42.94 ppm (d, 3P) (AA'A''BB'B'' system); UV/Vis ($1.25 \cdot 10^{-4}$ M, CH_2Cl_2): λ (ϵ) = 329 (10375), 278 nm ($16535 \text{ mol}^{-1} \cdot \text{dm}^3 \cdot \text{cm}^{-1}$); ESI-MS (CH_2Cl_2 , 20 V) m/z: 1838.8 $[\text{M}]^+$; elemental analysis calcd (%) for $\text{W}_3\text{S}_4\text{Br}_4\text{P}_6\text{C}_{61}\text{H}_{92}$: C 36.44, H 4.61; found: C 36.50, H 5.20; CD ($1.20 \cdot 10^{-4}$ M, CH_2Cl_2) λ (mdeg): 530 (-36), 432 (-22), 404 (-50), 365 (119), 328 (132), 295 (17), 262 nm (201)

2.3. X-ray data collection and structure refinement

Suitable crystals for X-ray studies of $[M\text{-}1]\text{Br}$ were grown by slow vapor diffusion of toluene into a sample solution of $[M\text{-}1]\text{Br}$ in CH_2Cl_2 or diethyl ether into sample solutions of $[P\text{-}2]\text{PF}_6$ and $[P\text{-}3]\text{Br}$ in CH_2Cl_2 . Crystal evaluation and diffraction data for compounds $[M\text{-}1]\text{Br}$ and $[P\text{-}3]\text{Br}$ were performed on an Agilent Supernova diffractometer equipped with an Atlas CCD detector using Mo- $\text{K}\alpha$ radiation ($\lambda = 0.71073 \text{ \AA}$). No instrument or crystal instabilities were observed during data

collection [34]. Absorption corrections based on the Gaussian method [35] for $M-1^+$ cluster and Multi-scan method [36] for $P-3^+$ cluster were applied. Diffraction data for $[P-2]PF_6$ was collected with a Bruker SMART CCD diffractometer using Mo-K α radiation ($\lambda = 0.71073 \text{ \AA}$) at $T = 296.15(2) \text{ K}$. The data were collected with a frame width of 0.3° in Ω and a counting time of 25 s per frame at a crystal–detector distance of 4 cm. Data reduction was carried out using the programme SAINT [37] and SADABS software [38] was used for absorption correction. Structure of $[M-1]Br$ was solved by charge-flipping methods using Superflip [39] while structures of $[P-2]PF_6$ and $[P-3]Br$ were solved by direct methods using SHELXS-97 [40] and refined by the full-matrix method based on F^2 with the program SHELXL-97 using the OLEX software package [41]. The graphics were performed with the Diamond visual crystal structure information system software [42]. For compound $[M-1]Br$, all atoms in the cluster cation as well as the Br anion were refined anisotropically. This salt crystallises with two CH_2Cl_2 and one toluene solvent molecules. One of the carbon atoms (C43) of dichloromethane molecule had to be refined isotropically. The carbon atoms of the toluene molecule were also refined isotropically and their bond distances were constrained to a fixed value of 1.36 \AA . For compounds $[P-2]PF_6$ and $[P-3]Br \cdot 2CH_2Cl_2$ all atoms were refined anisotropically. The H atoms in all three clusters were positioned geometrically, assigned isotropic thermal parameters and allowed to ride on their respective parent carbon atoms. Three top peaks of $ca. 5.32, 4.18$ and $3.1 \text{ e} \cdot \text{\AA}^{-3}$ remained in the last Fourier map of the $M-[W_3S_4Br_3((S,S)\text{-Me-BPE})_3]Br$ structure although these residual density were too close to the heavy atom ($ca. 0.86, 0.81$ and 0.9 \AA , respectively) to be included in the model. Flack parameter was refined and used to assess the absolute structure [43–45]. Crystal data and structure refinement information for all compounds are summarized in Table 1.

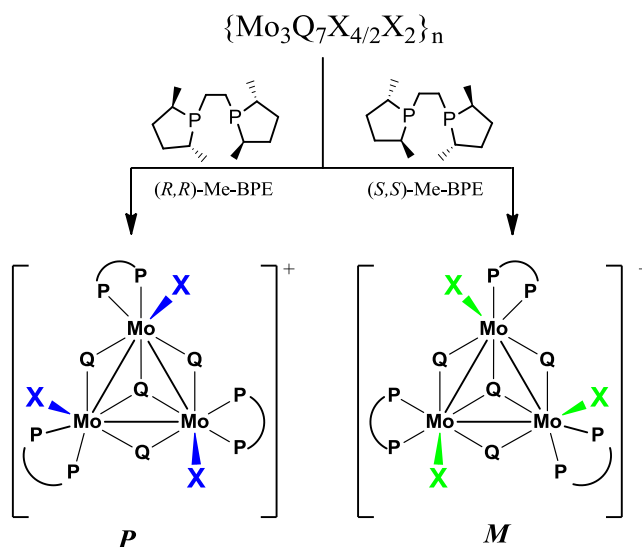
Table 1. Crystallographic data for M -[W₃S₄Br₃((*S,S*)-Me-BPE)₃]Br·2CH₂Cl₂·C₇H₈, [M -1]Br·2CH₂Cl₂·C₇H₈, P -[W₃Se₄Br₃((*R,R*)-Me-BPE)₃]PF₆, [P -2]PF₆, P -[W₃S₄Br₃((*R,R*)-DUPHOS)₃]Br·2CH₂Cl₂, [P -3]Br·2CH₂Cl₂.

	[M -1]Br·2CH ₂ Cl ₂ ·C ₇ H ₈	[P -2]PF ₆	[P -3]Br·2CH ₂ Cl ₂
Empirical formula	C ₅₁ H ₉₆ Br ₄ Cl ₄ P ₆ S ₄ W ₃	C ₄₂ H ₈₄ Br ₃ P ₇ Se ₄ W ₃ F ₆	C ₅₆ H ₈₈ Br ₄ Cl ₄ P ₆ S ₄ W ₃
Formula weight	2036.32	2027	2088.31
Temperature (K)	293(2)	296.15	200(2)
Crystal system	Monoclinic	Trigonal	Monoclinic
Space group	$P2_1$	$R3$	$P2_1$
<i>Unit cell dimensions</i>			
a , Å	11.9974(16)	15.6097(11)	12.02802(15)
b , Å	19.6767(3)	15.6097(11)	24.0309(3)
c , Å	14.8860(19)	23.225(3)	12.3079(3)
α ≡	90	90	90
β ≡	98.107(12)	90	93.6703(14)
γ ≡	90	120	90
Volume, Å ³	3473.21(8)	4900.9(10)	3557.28(9)
Z	2	3	2
D_{calc} (Mg m ⁻³)	1.947	2.060	1.950
Absorption coefficient (mm ⁻¹)	7.702	9.547	7.523
$F(000)$	1972.0	2874.0	2016.0
Crystal size (mm ³)	0.19 x 0.16 x 0.12	0.26 × 0.16 × 0.15	0.37 × 0.24 × 0.03
Theta range for data collection (°)	2.91-29.40	2.31-24.99	2.90-29.20
Index ranges	-15 ≤ h ≤ 16, -26 ≤ k ≤ 26, -20 ≤ l ≤ 19	-18 ≤ h ≤ 18, -18 ≤ k ≤ 18, -16 ≤ l ≤ 27	-15 ≤ h ≤ 16, -32 ≤ k ≤ 30, -16 ≤ l ≤ 16
Reflections collected	76264	9032	40359
Independent reflections	17297 [$R_{\text{int}} = 0.0368$]	3092 [$R_{\text{int}} = 0.0384$]	16591 [$R_{\text{int}} = 0.0595$]
Absorption correction	gaussian	Multi-scan	Multi-scan
Refinement method	full-matrix least-squares on F^2	full-matrix least-squares on F^2	full-matrix least-squares on F^2
Data/restraints/parameters	17297/8/622	3092/1/196	16591/1/706
Goodness-of-fit on F^2	1.043	1.123	1.051
Final R indices [$I > 2\sigma(I)$]	$R_1 = 0.0333$, $wR_2 = 0.0819$	$R_1 = 0.0322$, $wR_2 = 0.0838$	$R_1 = 0.0509$, $wR_2 = 0.1126$
R indices (all data)	$R_1 = 0.0358$, $wR_2 = 0.0840$	$R_1 = 0.0365$, $wR_2 = 0.0861$	$R_1 = 0.0670$, $wR_2 = 0.1271$
Largest difference in peak and hole (e·Å ⁻³)	5.32 and -1.77	1.50 and -1.35	2.10 and -2.10
Flack parameter	-0.016(3)	0.032(13)	-0.015(7)

3. Results and discussion

3.1. Synthesis and characterization

Nowadays, excision reaction of $\{\text{M}_3\text{Q}_7\text{X}_{4/2}\text{X}_2\}_n$ polymeric phases is considered as a rational and well-established procedure to prepare cuboidal cubane-type clusters with backbone chirality. This synthetic methodology requires the presence of species with high affinity for chalcogen atoms, *i.e.* phosphines, to make feasible the dimensional reduction. As already mentioned in the introduction, racemic mixtures are invariably obtained when non-chiral diphosphines are employed as dimensional reducing agents. Interestingly, the reaction showed a unique efficiency and stereoselectivity when $\{\text{Mo}_3\text{S}_7\text{Cl}_{4/2}\text{Cl}_2\}_n$ phases are reacted with chiral diphosphines, namely *(R,R)*-Me-BPE or *(S,S)*-Me-BPE, to afford the trinuclear *P*- $[\text{Mo}_3\text{S}_4\text{Cl}_3((R,R)\text{-Me-BPE})_3]^+$ and *M*- $[\text{Mo}_3\text{S}_4\text{Cl}_3((R,R)\text{-Me-BPE})_3]^+$ stereoisomers [7], respectively, as represented in Scheme 2. This synthetic procedure has been extended to the bromine and selenium analogues and, more recently, the trimetallic *P*- $[\text{W}_3\text{S}_4\text{Br}_3((R,R)\text{-Me-BPE})_3]^+$ complex was also isolated. [18]



Scheme 2

To validate the generality of this synthetic strategy, we have reacted the *(S,S)*-Me-BPE diphosphine with $\{\text{W}_3\text{S}_7\text{Br}_{4/2}\text{Br}_2\}_n$ and the *M*- $[\text{W}_3\text{S}_4\text{Br}_3((R,R)\text{-Me-BPE})_3]^+$ (*M-1*⁺) diastereoisomer has been characterized as the only reaction product. The absolute configuration of *M-1*⁺ as *M* has been determined by X-ray crystallography, as detailed in the following section. The enantiomeric character of *M-1*⁺ with regard to the *P*- $[\text{W}_3\text{S}_4\text{Br}_3((S,S)\text{-Me-BPE})_3]^+$ cation has been proved by CD

measurements, shown in Figure 1. Compound $M-1^+$ displays three signals at $\lambda_{\max} = 270, 325$ and 404 nm associated to $-132, -88$ and $+62$ mdeg with similar intensities, but opposite signs to those produced by the $P-[W_3S_4Br_3((R,R)\text{-Me-BPE})_3]^+$ complex giving support to the enantiomerism of the two complexes [18]. As expected, both compounds have the same ESI-MS and $P\{^1H\}$ -NMR spectra. The last one shows two double of doublets at $\delta = 31.65$ ppm (three P atoms) and at $\delta = 35.88$ ppm (three P atoms) and the typical satellites due to the coupling with the ^{183}W nuclei.

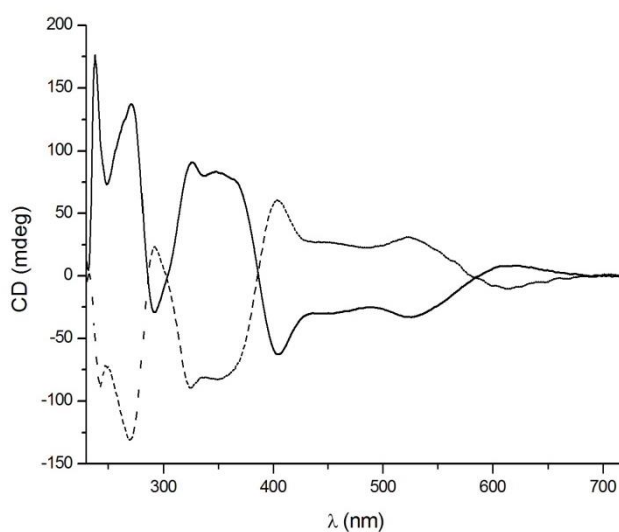
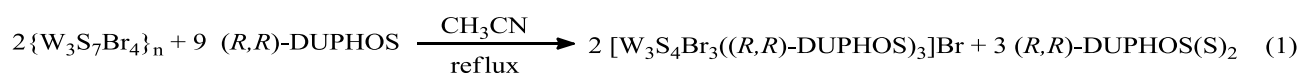


Figure 1. CD spectra of $P-[W_3S_4Br_3(\text{Me-BPE})_3]^+$ (—) and $M-1^+$ (---) enantiomers in dichloromethane at 25°C at $1.13 \cdot 10^{-4}$ M and $1.15 \cdot 10^{-4}$ M, respectively.

As previously observed for the molybdenum system, reaction of the selenium $\{W_3Se_7Br_4\}_n$ phase with (R,R) -Me-BPE in boiling acetonitrile affords the optically pure $P-[W_3Se_4Br_3((R,R)\text{-Me-BPE})_3]^+$ ($P-2^+$) cation in quantitative yields while their sulfur analogues were only obtained in moderate yields, *ca.* 50 %. Again, X-ray crystallography (see *vide infra*) and CD spectroscopy give support to the absolute configuration of this complex as P . At this point, we decided to investigate whether the stereoselectivity of the excision of polymeric $\{W_3Q_7X_{4/2}X_2\}_n$ phases could be extended to other diphosphines. With this idea in mind, we carried out the excision reaction between $\{W_3S_7Br_4\}_n$ in the presence of an excess of (R,R) -DUPHOS according to equation (1).



After purification of the reaction mixture, $^{31}\text{P}\{^1\text{H}\}$ -NMR spectroscopy and ESI-MS spectrometry indicate the presence of a unique diastereoisomer, unequivocally identified as *P*- $[\text{W}_3\text{S}_4\text{Br}_3((R,R)\text{-Me-DUPHOS})_3]^+$ (*P-3*⁺), as detailed as follows. CD spectrum of *P-3*⁺ showed Cotton effects at $\lambda_{\text{max}} = 404$ (-50), 365 (119), 328 (132), 262 nm (201 mdeg) with the same tendency in signs as *P-2*⁺ and the reported *P*- $[\text{W}_3\text{S}_4\text{Br}_3((R,R)\text{-Me-BPE})_3]^+$ complex, giving support to its absolute configuration as *P*. Nevertheless, X-ray diffraction measurements were carried out in order to ascertain the stereochemistry observed by CD solution techniques and refinement of Flack parameter determined unequivocally the stereochemistry of the cluster in [*P-3*]Br compound. Finally, CD spectra analysis of *M-1*⁺, *P-2*⁺ and *P-3*⁺ compounds revealed only small and subtle differences, being the most remarkable a slight displacement to the red region on going from sulfur to selenium. Therefore, the maximum peaks in the CD spectra for the whole tungsten family clusters issued in this report are displaced to the blue region when compared to the molybdenum analogues.

3.2. Crystal structure description

The crystal structures of the bromide salts of *M-1*⁺ and *P-3*⁺ and the hexafluorophosphate salt of *P-2*⁺ were determined by single-crystal X-ray diffraction. As expected, all three compounds crystallised in non-centrosymmetric space groups, namely, monoclinic *P2*₁ for [*M-1*]Br and [*P-3*]Br, and trigonal *R3* for [*P-2*]PF₆. An ORTEP view of the *P-2*⁺ and *P-3*⁺ cations is shown in Figure 2. Selected bond distances for [*M-1*]Br, [*P-2*]PF₆ and [*P-3*]Br are listed in Table 2 together with those reported for the *P*- $[\text{W}_3\text{S}_4\text{Br}_3((R,R)\text{-Me-BPE})_3]^+$ cation for comparative purposes. The three clusters possess an incomplete cuboidal W_3Q_4 core in which the tungsten atoms define an equilateral triangle with two phosphorus atoms of the diphosphine ligand and one bromine atom occupying the outer positions. In all cases, the uniform stereochemistry of the diphosphine ligands as (*R,R*) or (*S,S*) was observed with no ambiguity. Flack parameters around zero for all three absolute structures has allowed us to unequivocally assess the stereochemistry of *M-1*⁺ as *M* and *P-2*⁺ and *P-3*⁺ as *P*.

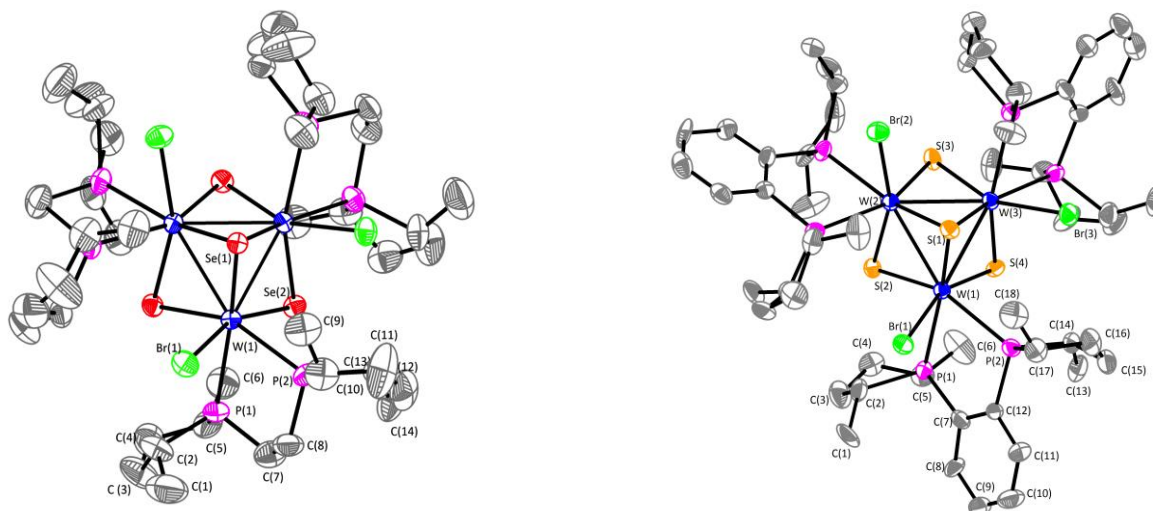


Figure 2. ORTEP representation (50% probability ellipsoids) of the cationic clusters P - $[W_3Se_4Br_3((R,R)\text{-Me-BPE})_3]^+$, $P\text{-}2^+$ and P - $[W_3S_4Br_3((R,R)\text{-DUPHOS})_3]^+$, $P\text{-}3^+$, respectively, with the atom-numbering scheme. Hydrogen atoms have been omitted for clarity.

Table 2. Selected bond distances (Å) for $[M\text{-}1]Br$, $[P\text{-}2]Br$ and $[P\text{-}3]PF_6$.

	$[W_3S_4Br_3((R,R)\text{-Me-BPE})_3](PF_6)^{[18]}$	$[M\text{-}1]Br^a$	$[P\text{-}2]PF_6$	$[P\text{-}3]Br^a$
W-W	2.793[4]	2.7897[5]	2.8670(8)	2.8102[8]
W- μ_3 -Q(1)	2.371[4]	2.3637[2]	2.4849(18)	2.3737[4]
W- μ -Q(2) ^b	2.289[5]	2.2893[2]	2.4111(13)	2.293[4]
W- μ -Q(2) ^c	2.311[6]	2.3163[2]	2.4498(13)	2.3133[4]
W-P(1) ^d	2.559[3]	2.552[2]	2.564(4)	2.553[4]
W-P(2) ^e	2.633[7]	2.6243[2]	2.653(4)	2.6217[4]
W-Br	2.6303[2]	2.6296[10]	2.6313(15)	2.6247[17]

^a Standard deviations for averaged values are given in square brackets. ^b W- μ -Q distance *trans* to W-Br bond. ^c W- μ -Q distance *cis* to W-Br bond. ^d Distance *trans* to the W-(μ_3 -Q) bond. ^e Distance *cis* to the W-(μ_3 -Q) bond.

Metal-metal bond distances in M - $[W_3S_4Br_3((S,S)\text{-Me-BPE})_3]^+$ and P - $[W_3S_4Br_3((R,R)\text{-DUPHOS})_3]^+$ range between 2.79 - 2.81 Å, which agrees with the presence of a single W-W bond and a +4 oxidation state for the tungsten atoms. The intermetallic bond length increases in the P - $[W_3Se_4Br_3((R,R)\text{-Me-BPE})_3]^+$ selenide cluster up to 2.87 Å, in agreement with the larger covalent radius of selenium atom. The same tendency is observed in the W-(μ_3 -Q) and W-(μ -Q) bond distances, which elongate *ca.* 0.13 Å when sulfur is replaced by selenium. Differences in the non-equivalent W-(μ -Q) bond lengths are attributed to the *trans* effect of the bromine *versus* the

phosphorus atoms of the diphosphine ligand. Finally, replacement of the diphosphine, Me-BPE by DUPHOS, has not significant effect on the complex bond lengths.

At present, the reasons behind the stereochemistry of this synthetic route are not clear although factors such interionic interactions and steric hindrance may have their influence. However, it seems clear that once the chirality of one metal center is defined, that of the other two is equally fixed.

4. Conclusions

Enantioselective synthesis of chiral group six $[M_3Q_4X_3(\text{diphosphine})_3]^+$ cluster complexes by excision of one dimensional $\{M_3Q_7X_4\}_n$ polymers using chiral phosphines has been extended to other cluster cores, namely W_3Se_4 and other diphosphines such as (*R,R*)-DUPHOS. This work confirms that chirality transfer from optically pure organic ligands to polymeric inorganic phases is a good and simple alternative to prepare enantiomerically pure C_3 symmetry cluster complexes with backbone chirality in good yields. In all cases investigated, excision reactions using (*R,R*)-Me-BPE and (*R,R*)-DUPHOS diphosphines afford the *P*- M_3Q_4 stereoisomer while its *M*- M_3Q_4 enantiomer is invariably obtained when using (*S,S*)-diphosphines. The cuboidal geometry of the cluster core with a missing metal atom makes these complexes excellent candidates as potential metalloligands able to coordinate a second transition metal and afford enantiopure cubane-type $M_3M'Q_4$ complexes.

Supplementary material

CCDC-1008234 (*[M-1]*Br), CCDC-1008232 (*[P-2]*PF₆) and CCDC-1008233 (*[P-3]*Br) contain the supplementary crystallographic data for this paper. These data can be obtained free of charge from the Cambridge Crystallographic Data Centre via www.ccdc.cam.ac.uk/data_requested/cif

Acknowledgements

The financial support of the Spanish Ministerio de Economía y Competitividad (grants CTQ2011-23157), Universitat Jaume I (research project P1.1B2013-19) and Generalitat Valenciana (Prometeo/2009/053 and ACOMP/2013/215) is gratefully acknowledged. The authors also thank the Serveis Central d'Instrumentació Científica (SCIC) of the Universitat Jaume I for providing us with the mass spectrometry, NMR, circular dichroism and X-ray facilities.

References

- [1] Yang, K. Y.; Haynes, C. A.; Spatzal, T.; Rees, D. C.; Howard, J. B., *Biochemistry*, (2014) **53**, 333.
- [2] Herbst, K.; Brorson, M.; Carlsson, A., *Journal of Molecular Catalysis a-Chemical*, (2010) **325**, 1.
- [3] Kogan, V. M.; Nikulshin, P. A.; Rozhdestvenskaya, N. N., *Fuel*, (2012) **100**, 2.
- [4] Bahn, C. S.; Tan, A.; Harris, S., *Inorg. Chem.*, (1998) **37**, 2770.
- [5] Takei, I.; Wakebe, Y.; Suzuki, K.; Enta, Y.; Suzuki, T.; Mizobe, Y.; Hidai, M., *Organometallics*, (2003) **22**, 4639.
- [6] Takei, L.; Dohki, K.; Kobayashi, K.; Suzuki, T.; Hidai, M., *Inorg. Chem.*, (2005) **44**, 3768.
- [7] Feliz, M.; Guillamon, E.; Llusar, R.; Vicent, C.; Stiriba, S. E.; Perez-Prieto, J.; Barberis, M., *Chem.-Eur. J.*, (2006) **12**, 1486.
- [8] Guillamon, E.; Llusar, R.; Perez-Prieto, J.; Stiriba, S. E., *J. Organomet. Chem.*, (2008) **693**, 1723.
- [9] Beltran, T. F.; Feliz, M.; Llusar, R.; Mata, J. A.; Safont, V. S., *Organometallics*, (2011) **30**, 290.
- [10] Sorribes, I.; Wienhofer, G.; Vicent, C.; Junge, K.; Llusar, R.; Beller, M., *Angewandte Chemie-International Edition*, (2012) **51**, 7794.
- [11] Larionov, S. V.; Myachina, L. I.; Romanenko, G. V.; Tkachev, A. V.; Sheludyakova, L. A.; Ikorskii, V. N.; Boguslavskii, E. G., *Russian Journal of Coordination Chemistry*, (2001) **27**, 423.

- [12] Shabalina, I. Y.; Kirin, V. P.; Maksakov, V. A.; Virovets, A. V.; Golovin, A. V.; Agafontsev, A. M.; Tkachev, A. V., *Russian Journal of Coordination Chemistry*, (2008) **34**, 286.
- [13] Salomon, C.; Dal Molin, S.; Fortin, D.; Mugnier, Y.; Boere, R. T.; Juge, S.; Harvey, P. D., *Dalton Transactions*, (2010) **39**, 10068.
- [14] Estevan, F.; Feliz, M.; Llusar, R.; Mata, J. A.; Uriel, S., *Polyhedron*, (2001) **20**, 527.
- [15] Feliz, M.; Llusar, R.; Uriel, S.; Vicent, C.; Humphrey, M. G.; Lucas, N. T.; Samoc, M.; Luther-Davies, B., *Inorg. Chim. Acta*, (2003) **349**, 69.
- [16] Algarra, A. S. G.; Basallote, M. G.; Fernandez-Trujillo, M. J.; Llusar, R.; Safont, V. S.; Vicent, C., *Inorg. Chem.*, (2006) **45**, 5774.
- [17] Algarra, A. G.; Basallote, M. G.; Fernandez-Trujillo, M. J.; Guillamon, E.; Llusar, R.; Segarra, M. D.; Vicent, C., *Inorg. Chem.*, (2007) **46**, 7668.
- [18] Algarra, A. G.; Basallote, M. G.; Fernandez-Trujillo, M. J.; Feliz, M.; Guillamon, E.; Llusar, R.; Sorribes, I.; Vicent, C., *Inorg. Chem.*, (2010) **49**, 5935.
- [19] Basallote, M. G.; Fernandez-Trujillo, M. J.; Pino-Charnorro, J. A.; Beltran, T. F.; Corao, C.; Llusar, R.; Sokolov, M.; Vicent, C., *Inorg. Chem.*, (2012) **51**, 6794.
- [20] Beltran, T. F.; Feliz, M.; Llusar, R.; Safont, V. S.; Vicent, C., *Eur. J. Inorg. Chem.*, (2013) **2013**, 5797.
- [21] Avarvari, N.; Kirakci, K.; Llusar, R.; Polo, V.; Sorribes, I.; Vicent, C., *Inorg. Chem.*, (2010) **49**, 1894.
- [22] Katsuki, T.; Sharpless, K. B., *J. Am. Chem. Soc.*, (1980) **102**, 5974.
- [23] Knowles, W. S.; Sabacky, M. J., *Chem. Commun.*, (1968), 1445.
- [24] Ohta, T.; Takaya, H.; Noyori, R., *Inorg. Chem.*, (1988) **27**, 566.
- [25] Campian, M. V.; Perutz, R. N.; Procacci, B.; Thatcher, R. J.; Torres, O.; Whitwood, A. C., *J. Am. Chem. Soc.*, (2012) **134**, 3480.
- [26] Meggers, E., *Eur. J. Inorg. Chem.*, (2011), 2911.
- [27] Crassous, J., *Chem. Soc. Rev.*, (2009) **38**, 830.
- [28] Constable, E. C., *Chem. Soc. Rev.*, (2013) **42**, 1637.

- [29] Frantz, R.; Guillamon, E.; Lacour, J.; Llusar, R.; Polo, V.; Vicent, C., *Inorg. Chem.*, (2007) **46**, 10717.
- [30] Llusar, R.; Uriel, S., *Eur. J. Inorg. Chem.*, (2003), 1271.
- [31] Cotton, F. A.; Kibala, P. A.; Matusz, M.; McCaleb, C. S.; Sandor, R. B. W., *Inorg. Chem.*, (1989) **28**, 2623.
- [32] Fedin, V. P.; Sokolov, M. N.; Myakishev, K. G.; Gerasko, O. A.; Fedorov, V. Y.; Macicek, J., *Polyhedron*, (1991) **10**, 1311.
- [33] MASSLYNX, e. W. L. M., MA, 2005,
- [34] Agilent, *CrysAlisPro version 171.36.24; Agilent Technologies, Santa Clara, CA, 2012*
- [35] Busing, W. R.; Levy, H. A., *Acta Crystallographica*, (1957) **10**, 180.
- [36] Clark, R. C.; Reid, J. S., *Acta Crystallographica Section A*, (1995) **51**, 887.
- [37] Bruker Analytical X-Ray Systems:Madison, W., SAINT, In (2001).
- [38] Scheldrick, G. M., *SADABS*, Göttingen, (1996).
- [39] Palatinus, L.; Chapuis, G., *J. Appl. Crystallogr.*, (2007) **40**, 786.
- [40] Sheldrick, G. M., *Acta Crystallographica Section A*, (2008) **64**, 112.
- [41] Dolomanov, O. V.; Bourhis, L. J.; Gildea, R. J.; Howard, J. A. K.; Puschmann, H., *J. Appl. Crystallogr.*, (2009) **42**, 339.
- [42] Brandenburg, K.; Putz, H., *Crystal Impact, GbR, Bonn, Germany*, (2006),
- [43] Flack, H. D., *Acta Crystallographica Section A*, (1983) **39**, 876.
- [44] Bernardinelli, G.; Flack, H. D., *Acta Crystallographica Section A*, (1985) **41**, 500.
- [45] Flack, H. D.; Bernardinelli, G., *Acta Crystallographica Section A*, (1999) **55**, 908.